American Mineralogist, Volume 68, pages 554–565, 1983

Exsolution and crystal chemistry of the sodium mica wonesite

DAVID R. VEBLEN

Department of Earth and Planetary Sciences
The Johns Hopkins University
Baltimore, Maryland 21218

Abstract

Transmission electron microscopy, electron diffraction, and X-ray analytical electron microscopy indicate that the sodium mica wonesite from the Post Pond Volcanics, Vermont, has partially exsolved to a lamellar intergrowth of talc and a sodium mica having fewer interlayer site vacancies than the initial wonesite. This is the first known example of exsolution in a mica. The mica is enriched in Na, Al, K, Ti, Cr, and Fe relative to the talc. The lamellae, the wavelength of which varies from a few hundred ångströms up to about 0.5 μm, are inclined to the layers of the mica and talc structures at a variable angle that averages about 37°. This microstructure explains why wonesite is not expandable in water, unlike a number of other natural and synthetic sodium micas and smectites.

A new method of deriving the chemical compositions of the phases in fine lamellar intergrowths from electron microscope X-ray analyses is described. The method, which utilizes the bulk chemical analysis of the intergrowth as a standard, is used to derive the chemical compositions of the intergrown talc and mica. These analyses clarify the shape of the talc-wonesite miscibility gap, which is strongly asymmetric and skewed toward talc. In addition to clarifying the phase relations of the sodium micas, the exsolution of wonesite provides a structural analogy for amphibole exsolution phenomena that involve the amphibole A-site. The study clearly demonstrates that wonesite is a valid mineral species. However, the solid solution ranges exhibited by sodium micas suggest that the nomenclature used to describe them should be clarified.

Introduction

The recently-discovered mica mineral wonesite is a sodium-rich biotite with substantial tschermaks substitution (Spear *et al.*, 1981). The contents of the interlayer sites in this mineral, as deduced from electron microprobe analyses, are approximately $Na_{0.40}K_{0.07}\square_{0.53}$, where $\square$ represents a vacancy (Spear *et al.*, 1981). Wonesite therefore has a very low interlayer charge compared to other micas and, like smectites, should be expandable in water and ethylene glycol. Wonesite is not expandable, however, suggesting that it might consist of a disordered submicroscopic mixed-layer intergrowth of Na-biotite and talc on (001), for example, or that the chemical analysis is incorrect. To resolve this problem, the transmission electron microscopy (TEM) study described in this paper was undertaken. The results show that wonesite in most places is not a mixed-layer mineral, although local disordered mixing of mica with chlorite and kaolinite does occur, and most wonesite contains small numbers of intercalated brucite-like layers, which produce isolated chlorite-like structural configurations. Instead, wonesite has exsolved pervasively to a lamellar mixture of Na-biotite and talc, providing us with the first clear example of exsolution in a mica. Thus, under metamorphic conditions, wonesite must be a valid homogeneous mineral. Furthermore, analytical TEM indicates that the mica portion of the intergrowth still contains substantial numbers of interlayer site vacancies, so that it should be considered to be wonesite as well.

In the present paper, the structural and chemical details of the exsolution microstructure in wonesite are considered. Wonesite hydration properties are compared with those of other sodium micas. The nomenclature of sodium-rich micas is discussed in light of the chemical behavior of wonesite, and the relationships among exsolution phenomena in pyroxenes, amphiboles, and micas are considered.

In a companion paper (Veblen, 1983), other microstructures in wonesite and the other sheet silicates with which it coexists are described. These include polytypic variations, stacking disorder, twinning, low-angle grain boundaries, and the intergrowth of mica with chlorite, potassium biotite, and kaolinite. Although it is conceivable that some of the mixed layering phenomena are in some way related to exsolution, their origin remains unclear. The obvious exsolution features presented in the present paper have therefore been treated apart from these other phenomena. However, the reader should be aware of the

0003–004X/83/0506–0554$02.00

other complex structural problems associated with the sheet silicate assemblage in these Post Pond rocks, as described by Veblen (1983).

Specimens, experimental techniques, and image interpretation

The specimen used in this study was kindly supplied by Dr. Frank S. Spear (#68-432E). Its mineralogy, petrology, and chemistry have been thoroughly described by Spear *et al.* (1981). Some TEM specimens were prepared by ion milling of petrographic thin sections that had been cut normal to the rock foliation and mounted on Cu grids. They were lightly carbon coated. Other specimens were prepared by crushing and deposition on holey carbon TEM grids.

Electron microscopy and chemical analysis were performed with a Philips 400T microscope equipped with a Tracor Northern TN2000 energy-dispersive X-ray analyzer. All analyses were qualitative in the sense that thin film standards were not employed, but they were performed under similar conditions of specimen thickness and tilt to facilitate comparisons among different spectra.

Interpretation of the high-resolution TEM (HRTEM) images presented here and by Veblen (1983) largely follows that employed previously (Veblen and Buseck, 1979, 1980, 1981; Veblen, 1980; Iijima and Buseck, 1978; Buseck and Veblen, 1981). During the time when this work was performed, a technical difficulty with the microscope caused the resolution to be degraded, so that in most cases only the 00*l* diffractions were imaged. Most images were recorded at an underfocus of about 1000Å. In their extensive calculations of image contrast in various mica polytypes, Amouric *et al.* (1981) found that under certain imaging conditions, the apparent layer thicknesses in HRTEM images did not match those in the real crystal. Such anomalous spacings were observed experimentally in the present study, but only in relatively thick parts of mica specimens where stacking disorder is present. Near the thin edges, the mica layers in the images are invariably evenly spaced, so that interpretations based on (00*l*) fringe spacings are presumably correct. It is also probable that the spacing variations noted by Amouric *et al.* (1981) are not only a function of specimen thickness, but also are exacerbated by the contributions of diffracted beams other than 00*l* to the images. Layer thickness variations in chlorite images are discussed in more detail by Veblen (1983).

Exsolution microstructures

Of the two TEM specimens that were examined in this study, one exhibited alternating lamellae throughout the wonesite, as shown in Figure 1. The hole in this specimen, around the edges of which the observations were made, was approximately one millimeter in diameter; almost all of the material adjacent to the hole was wonesite, with minor amounts of K-biotite, as determined by X-ray analysis. Thus, a reasonably large amount of wonesite was examined in this specimen, and all of it contained this lamellar microstructure. In the second specimen, only minor amounts of wonesite were available for TEM observations; lamellar intergrowth as obvious as that shown in Figure 1 was not observed in this specimen, although phase separation on a finer scale and other interesting microstructures were present (Veblen, 1983).

Identification of the lamellae

Electron diffraction patterns from the intergrowth show that the 00*l* diffractions are split into two peaks that are indicative of (001) spacings of approximately 9.6Å and 9.3Å, consistent with d_{001} of Na-biotite (or wonesite) and talc respectively (Fig. 2). Qualitative X-ray analyses that were performed on adjacent lamellae to ensure essentially the same analytical conditions are shown in Figure 3. These analyses confirm the identification of the two sets of lamellae as Na-biotite and talc. The talc is significantly lower in Na, Al, K, Ti, Cr, and Fe than the biotite. In addition to the peaks from Na, Mg, Al, Si, K, Ti, Cr, and Fe, which were all observed in microprobe analyses of Spear *et al.* (1981), the TEM analyses show minor contamination peaks from Ar, which was presumably embedded in the minerals during ion milling, and Cu, which results from slight electron and X-ray irradiation of the specimen grid. The absence of the Ag *K* line confirmed that the Ar peak was, indeed, from Ar, rather than being the *L* line of Ag.

Physical description of the lamellar microstructure

The wavelength of the lamellar intergrowth varies in different parts of the specimen from about 0.5 μm down to a few hundred ångströms. In Figure 1 the lamellar wavelength is about 0.3 μm. Figure 1 also exhibits other important features. The talc lamellae contain numerous lenticular light areas where the layers of the structure have parted; these are discussed in more detail in the section "Diffraction details and lamellar misfits." Most important, Figure 1 shows that the talc-mica lamellae are inclined to the (001) layers of the structures, which are horizontal. The angle between the plane of exsolution and (001) was determined by high-angle tilting experiments in which the crystal was rotated around c^*. In such an experiment, the maximum observed angle is the true angle between the two planar features; this angle is about 37° in most parts of the specimen.

Unlike the planar lamellae in the area of Figure 1, the lamellae in some areas are curved and discontinuous, as shown in Figure 4. The angle between such lamellae and (001) is obviously variable. Some of the lamellae in Figure 4 have a distinct "$\int$" shape or curve at one of their ends. This is reminiscent of the curvature of exsolution lamellae in some clinopyroxenes, which apparetly results from growth of the lamellae during changing temperature and pressure conditions (Robinson *et al.*, 1977).

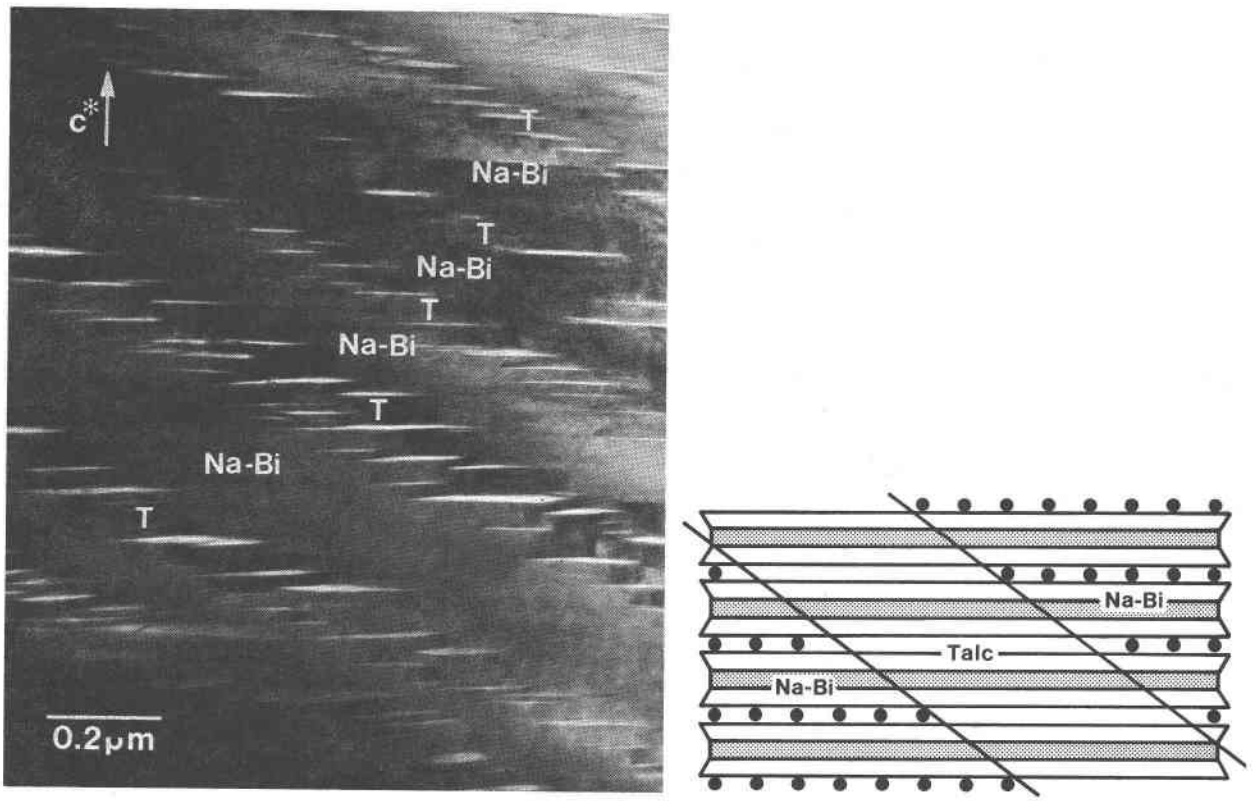

Fig. 1. a. Low-resolution bright-field electron micrograph of the lamellar microstructure in wonesite. Talc ("T") and sodium biotite ("Na–Bi") lamellae are tilted with respect to the plane (001), which is horizontal. The talc lamellae can be recognized by the white, lenticular voids parallel to (001). b. Schematic diagram of this microstructure, emphasizing that the lamellae are not parallel to the structural layers. Circles represent interlayer alkali sites.

Since the lamellae of talc in Na-biotite are inclined to the mica layers, they can also be observed in crushed specimens in which the viewing direction is normal to the layers. Figure 5 shows such a view, in which the specimen was tilted so that c^* was a few degrees away from the axis of the TEM to enhance contrast. Again, the lamellae were identified by X-ray analysis and can be seen to be discontinuous; there is slight curvature at the tips of some of them. The pronounced striping that cuts across the lamellae in part of Figure 5 is a moiré effect, discussed by Veblen (1983).

Orientation and origin of the lamellar microstructure

By combining the orientation information from images taken both normal to and parallel to the mica layers, the approximate three-dimensional orientation of the lamellae can be derived. The average orientation is apparently irrational and is close to {269} or {13$\bar{5}$} (there is an ambiguity in orientation resulting from poor quality of diffraction patterns from the exsolved crystal, the presence of twinning and stacking disorder, and the resulting inability to relate the orientation of the lamellae to a^* in the images taken parallel to the mica layers).

One observation that is not understood is why only one set of lamellae was observed in the wonesite. If the wonesite were a structurally-ordered monoclinic crystal, then two symmetry-related sets of lamellae would be expected (close to (269) and (2$\bar{6}$9), for example). Still more lamellar orientations would be expected because the wonesite crystals are heavily twinned and stacking-disordered. This situation is similar to the case of calcian dolomites, in which ordering of cations takes place parallel to only one of several symmetry-equivalent planes (Reeder, 1981). One possible explanation in the present case is that the precursor of the intergrowth, like talc, is triclinic. Another possibility is that a non-hydrostatic stress environment favored one orientation over the others.

The alternating lamellae of talc and Na-biotite almost certainly originated by exsolution from an initially homogeneous wonesite. Another possibility is that the lamellae originated by alteration, but this is not likely for several reasons: (1) the talc lamellae are commonly discontinuous, some apparently being disc-shaped, whereas alteration lamellae are expected to be connected to the crystal grain boundaries or fractures, where they have access to altering fluids; (2) in many parts of the specimen, the

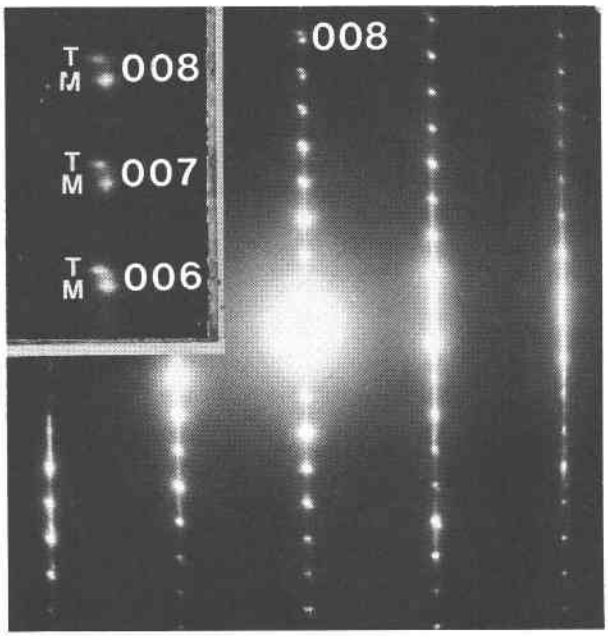

Fig. 2. Electron diffraction pattern of the talc-mica intergrowth. The inset in the upper left-hand corner is an enlarged view of the (006), (007), and (008) diffractions, which are clearly split. The talc and mica parts of these double reflections are labelled "T" and "M" respectively.

lamellae are spaced very evenly, as expected for exsolution but not alteration processes; (3) diffusion in sheet silicates is expected to be faster parallel to the layers than it is across the layers, so that lamellae resulting from alteration, which requires diffusion paths to the crystal environment, should be parallel to the layers. In wonesite, however, the lamellae are inclined to the mica layers, which would require diffusion through the layers if they formed by alteration. This microstructural evidence, combined with the fact that coexisting talc and Na micas demonstrate that there is, indeed, a miscibility gap between talc and Na-biotite (Spear *et al.*, 1981; Thompson, 1981; Schreyer *et al.*, 1980), makes exsolution the logical mechanism for the formation of the lamellar microstructure.

Although it is clear that the lamellae of talc and Na-biotite originated by exsolution, it is not so obvious why the lamellae are oriented as they are, approximately 37° from (001). One possibility is that the orientation is controlled solely by lattice misfit constraints, according to optimal phase boundary theory (Bollman, 1970; Robinson *et al.*, 1971, 1977; Jaffe *et al.*, 1975; Willaime and Brown, 1974; Tullis and Yund, 1979). This possibility is difficult to evaluate, however, because although the greatest metric misfits between the talc and Na-biotite structures are parallel to c^*, layer structures have large stiffness anisotropies, with the greatest compressibilities also parallel to c^* (Hazen and Finger, 1978a, b). The compressibility of potassium phlogopite, for example, is five times greater normal to the layers than it is parallel to the layers. The uncertainty in these large stiffness anisotropies precludes any reasonable evaluation of the least-energy lamellar orientation via optimal phase boundary theory in the case of wonesite.

Although structural misfit between the talc and biotite undoubtedly influences the orientation of the exsolution lamellae, it is also possible that kinetic factors are important in determining the orientation. To illustrate this possibility, let us suppose that the optimal phase boundaries are parallel to (001), so that the best fit between talc and biotite lamellae is obtained when the exsolution lamellae are parallel to (001). In this case, formation of the lamellae would require extensive diffusion of Na, Al, K, Fe, and other elements *through* the layers of the mica structure. The migration of large cations such as Na and K across the layers would surely require major structural disruption and might therefore be an extremely sluggish process. On the other hand, exsolution along planes that are inclined to (001) requires diffusion only parallel to the layers; presumably diffusion would take place primarily along the planes of the interlayer sites, which in the present case are half occupied by vacancies. Movement of Na and K would be entirely restricted to this plane, and other cations have rapid access to the interlayer from the tetrahedral and octahedral sheets. Such an exsolution process involving only cation migration parallel to the layers might be kinetically very favorable, compared to

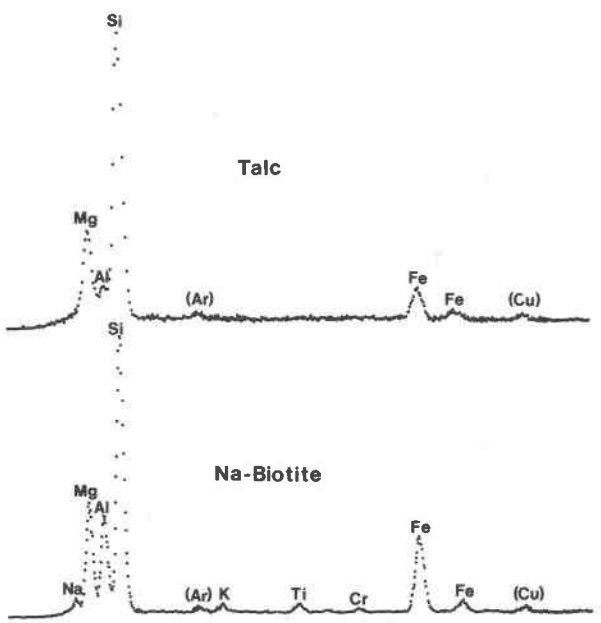

Fig. 3. Energy dispersive X-ray spectra of the talc (top) and Na-biotite lamella. The mica contains more Na, Al, K Ti, Cr, and Fe than the talc. Minor contamination peaks from Ar and Cu are present in both spectra.

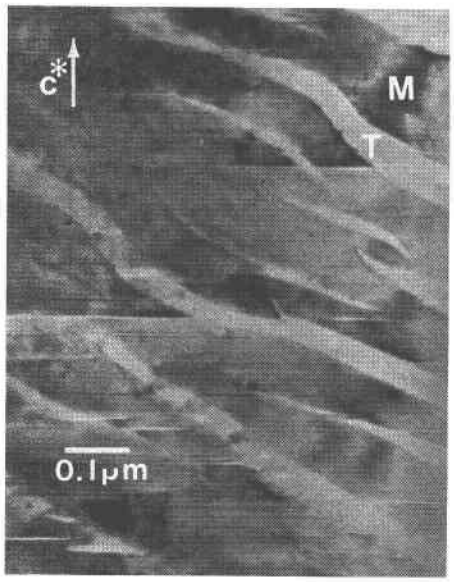

Fig. 4. Curved and terminating lamellae of talc ("T") in Na-biotite ("M"). The talc lamella exhibit lighter contrast because they have been rendered amorphous by the electron beam. The (001) plane is horizontal. (Bright-field image).

exsolution requiring major diffusion across the layers. Thus, even if the optimal phase boundaries are parallel to (001), kinetic factors might lead to exsolution lamellae in other orientations. Because the exsolution lamellae in wonesite are neither parallel to nor normal to (001), it may well be that the observed orientation is the result of a combination of lattice misfit constraints and kinetic factors.

Diffraction details and mechanisms of misfit accommodation

The electron diffraction pattern in Figure 2 contains several subtle features, some of which are relevant to the interpretation of structural details of the intergrowth of talc and Na-biotite. There are diffuse streaks between the pairs of (00*l*) diffractions; these could be related to disorder in the (00*l*) spacings in the crystal, but they instead could be simply the result of multiple diffraction from the (*hkl*) streaks that result from stacking disorder. The enhanced intensity between individual talc (T) and mica (M) diffraction spots, however, is probably related to the existence of spacings between those of talc and the Na-biotite.

High-resolution electron micrographs of the talc-mica intergrowths indicate that most of the TOT layers are continuous across the lamellae (Fig. 6), although in some places, interface dislocations consisting of terminating layers can be observed. Thus, the intergrowth is coherent in places and semi-coherent in others.

Because there is a difference in the spacings of the talc and mica layers (talc = 9.3Å; Na-mica = 9.6Å), there must be some mechanism in the coherent parts of the intergrowth that eliminates the misfit between the two structures. In most cases of lamellar intergrowths, misfit is minimized by adjusting the orientations of the structures and the interfaces, according to an optimal phase boundary theory (Bollman, 1970; Robinson *et al.*, 1971, 1977; Jaffe *et al.*, 1975; Willaime and Brown, 1974; Tullis and Yund, 1979). A cartoon illustrating such a mechanism is shown in Figure 7a, where the talc and Na-biotite layers are rotated with respect to each other; in this case, the interfaces were drawn normal to the mica layers for simplicity. Figure 7b shows another possible solution to the misfit problem that could operate in layer structures where the interlayer bonding is very weak. In this case, voids develop in the structure having the smaller interlayer spacing (in this case talc), and an average smaller spacing is achieved by bending the layers by varying amounts.

Theoretically, HRTEM studies of an intergrowth should resolve the question of which mechanism of misfit accommodation is operating. In practice, unfortuantely, extremely rapid electron radiation damage renders the talc amorphous in a few seconds, and such damage is even more severe in the neighborhood of the microstructures that would resolve the question. HRTEM results on the talc-mica intergrowths do show local rotation of the talc structure with respect to the mica in some places and bending of the talc layers in others, suggesting that both mechanisms may operate in different parts of the specimen. However, images of areas of undamaged material large enough to provide a clear answer could not be obtained. Local bending of layers can be seen by viewing Figure 6 at a low angle parallel to the layers.

Other lines of evidence also support the idea that both types of misfit accommodation occur in the wonesite specimen. Figure 1 is a low resolution micrograph in which white voids occur in the talc, supporting the mechanism of Figure 7b; such voids could, however, result from specimen deformation. In some electron diffraction patterns, a single c^* direction for talc indicates that the mechanism of Figure 7a may be operating. In other patterns, however, the (00*l*) diffractions of talc are arcuate, indicating that there is not a unique c^* direction and therefore that the talc layers are bent. These alternative lines of evidence are consistent with both mechanisms.

Chemical details and phase relations

There have been three recent reports of naturally-occurring sodium-rich trioctahedral micas (Spear *et al.*, 1978, 1981; Schreyer *et al.*, 1980; Keusen and Peters, 1980). The three different occurrences exhibit marked differences in interlayer occupancy and amount of tschermaks substitution ($Al_2Mg_{-1}Si_{-1}$), suggesting that a wide degree of chemical variability is possible in sodium micas. These chemical differences can be conveniently repre-

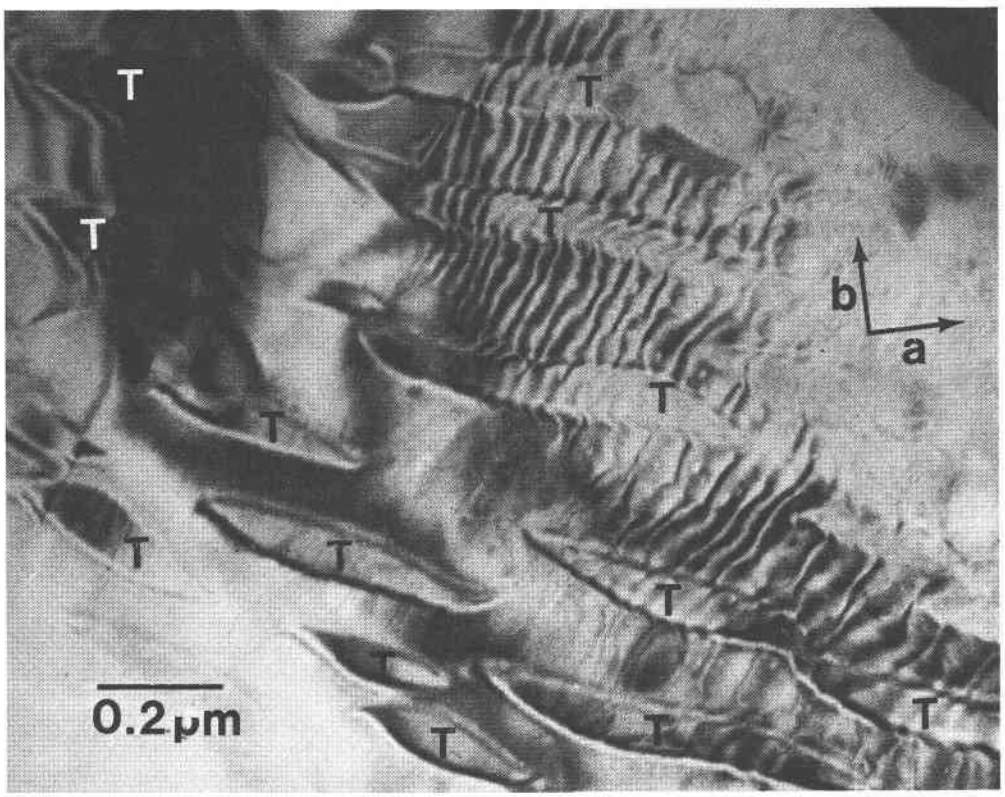

Fig. 5. The lamellar microstructure as viewed nearly normal to (001). The talc lamellae ("T") are discontinuous. (Bright-field image.)

sented on a ternary plot with the following vertices: (1) talc, $Mg_3[Si_4O_{10}](OH)_2$; (2) Na-phlogopite, $NaMg_3[AlSi_3O_{10}](OH)_2$; and (3) preiswerkite, $NaMg_2Al[Al_2Si_2O_{10}](OH)_2$. Phases can be plotted on such a diagram by condensing all interlayer cations to Na, all divalent octahedrally-coordinated cations to Mg, and all trivalent and tetravalent octahedrally-coordinated cations to Al. The talc vertex represents the structural compositional limit of empty interlayer sites, and the Na-phlogopite-preiswerkite join represents the structural limit of all

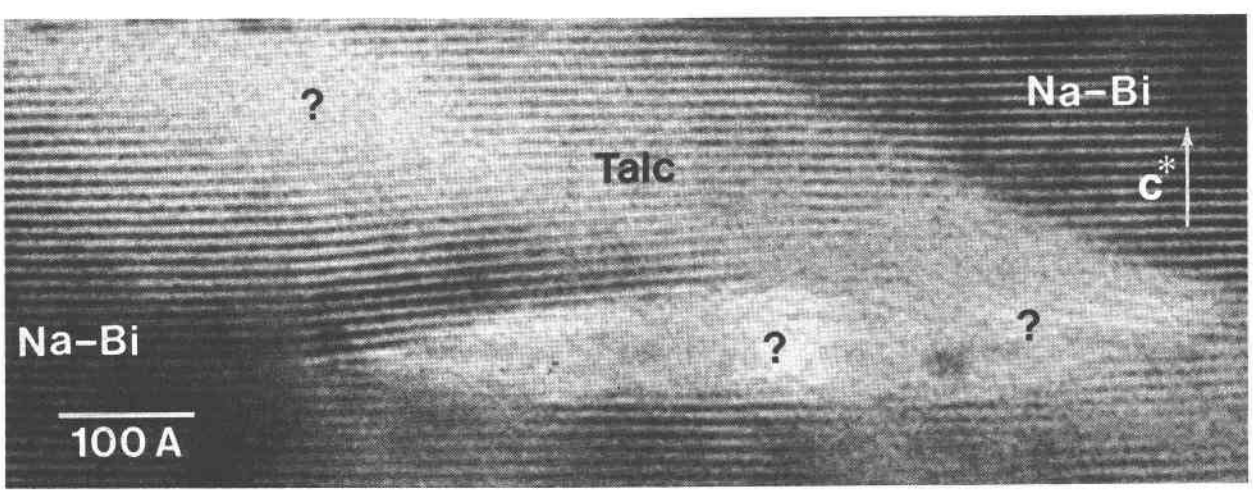

Fig. 6. High-resolution TEM image of a talc lamella in Na-biotite. The talc has slightly lighter contrast than the mica, and the lamellar interfaces, which run from upper left to lower right, are inclined to the silicate layers. Amorphous regions ("?") result from electron radiation damage, which occurs extremely rapidly.

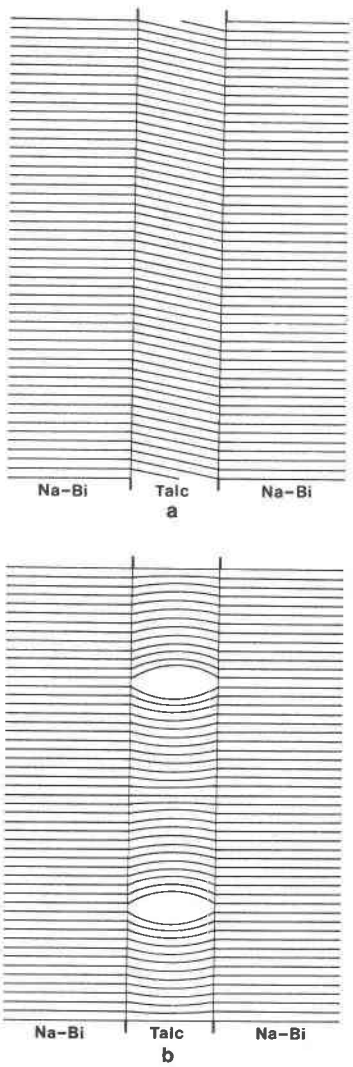

Fig. 7. (a) Schematic view of one way of absorbing the misfit between the mica ("Na–Bi") and talc structures. The lines represent the TOT silicate layers. In this case, the two structures are in different orientations, allowing for the smaller d_{001} of talc. The lamellar interfaces are drawn normal to the mica layers for simplicity. (b) Schematic view of an alternative way of absorbing the misfit between the mica and talc structures. In this case, lenticular voids have opened in the talc, and the talc layers have bent, allowing a smaller average d_{001} in the talc than in the mica.

interlayer sites full. The preiswerkite vertex represents a possible chemical limit of aluminum avoidance (more than two tetrahedrally coordinated Al per formula unit require Al–O–Al linkages, but see Hewitt and Wones, 1975), while the Na-phlogopite–talc join is the chemical limit of no tschermak's substitution.

Figure 8 shows the compositions of three naturally-occurring sodium micas and the talcs with which two of them coexist.[1] The preiswerkite of Keusen and Peters (1980) is very close to the ideal preiswerkite end member, having full interlayer sites and almost complete tschermak's substitution. The mica of Schreyer *et al.* (1980) is reasonably close to the Na-phlogopite end member, with limited tschermaks component and interlayer vacancies. The bulk composition of wonesite (Spear *et al.*, 1978, 1981) is closest to the talc vertex, by virtue of its large proportion of interlayer vacancies, but it also shows very substantial amounts of tschermaks substitution. Thus, wonesite cannot be thought of simply as a binary talc–Na-biotite solid solution, but must be considered as a talc–preiswerkite–Na-biotite ternary solution. In fact, wonesite is closer in composition to preiswerkite than it is to the Na-biotite end member. The compositions of the talcs coexisting with wonesite and the mica of Schreyer *et al.* (1980) suggest that more sodium-rich talcs may occur when there is less tschermaks substitution in the mica, as indicated by Thompson (1981). It is possible, however, that the difference in sodium contents of the talcs is also partially the result of different pressure conditions of metamorphism, for example, or that the talc of Schreyer *et al.* is a disordered mixed-layer talc-Na-phlogopite material; an electron microscopic study of this talc might clarify the question.

Analysis of the intergrowth and the talc–mica miscibility gap

In principle, it should be possible to illustrate the chemical characteristics of the exsolution in wonesite on a diagram such as that in Figure 8. However, the absence of quantitative microanalyses of the talc and mica lamellae would at first seem to preclude such a representation. To overcome the lack of the usual type of standarized thin-film analyses, a method of estimation of phase compositions for lamellar intergrowths has been devised. This method uses our knowledge of the relative volumes of the two phases, as derived from TEM images, and the bulk composition of the intergrowth, as derived from conventional analysis methods, such as electron microprobe. If we have a lamellar intergrowth of two phases α and β, with the volumes of the two phases equal to V_α and V_β and the normalized concentrations of some element in the two phases C_α and C_β, then

$$C_s = V_\alpha C_\alpha + V_\beta C_\beta$$

where C_s is the average concentration of the element in the mixture, as measured by a standard analytical tech-

[1] The structural formulae of the micas are (1) Spear *et al.*, 1981: $(Na_{0.395}K_{0.073}Ca_{0.002})(Mg_{2.195}Fe^{2+}_{0.389}Mn_{0.002}Cr_{0.004}Ti_{0.037}Al_{0.310})[Al_{0.767}Si_{3.233}O_{10}](OH,F)_2$; (2) Schreyer *et al.*, 1980: $(Na_{0.78}K_{0.05}Ca_{0.02})(Mg_{2.94}Al_{0.05}Ti_{0.02})[Al_{1.00}Si_{3.00}O_{10}](OH)_2$; (3) Keusen and Peters, 1980: $(Na_{0.98}K_{0.02}Ca_{0.01})(Mg_{1.91}Al_{0.91}Fe^{2+}_{0.08}Fe^{3+}_{0.06})[Al_{1.95}Si_{2.05}O_{10}](OH)_2$.

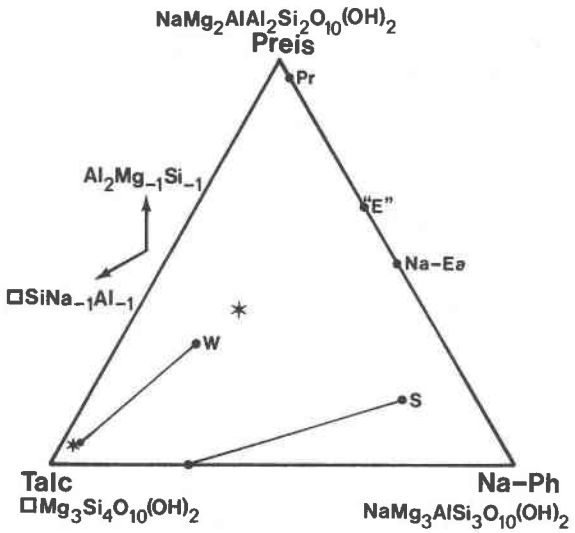

Fig. 8. The composition diagram talc–Na–phlogopite–preiswerkite, showing compositions of selected sodium micas. The exchange vectors (Thompson, 1981) $Al_2Mg_{-1}Si_{-1}$ and $SiNa_{-1}Al_{-1}$ are indicated. The averaged anlayses have been condensed by Mg = Mg + Fe^{2+} + Mn, Na = Na + Na + K + Ca, and Al = Al + Fe^{3+} + Cr + Ti; thus, $SiNa_{-1}Al_{-1}$ was taken as the proportion of vacancies in the interlayer sites, and $Al_2Mg_{-1}Si_{-1}$ was taken as the amount of tetrahedral Al minus (Na + K + Ca). The wonesite of Spear *et al.* (1981) ("W") and the Na-phlogopite of Schreyer *et al.* (1980) ("S") are connected by tie lines to the bulk talcs with which they coexisted, and "Pr" is the preiswerkite of Keusen and Peters (1980). The compositions marked "*" were derived for the exsolution lamellae in wonesite by X-ray analysis; these compositions are discussed in the text, as is the composition "E."

nique. Because $V_\beta = 1 - V_\alpha$,

$$C_s = V_\alpha C_\alpha - V_\alpha C_\beta + C_\beta$$

$$C_\beta = \frac{C_s}{V_\alpha(C_R - 1) + 1} \quad (1)$$

where $C_R = C_\alpha/C_\beta$. If X-ray spectra are collected from the two phases in a thin film, under the same analytical conditions, then the intensity ratio of the peaks for the element in question is also equal to C_R: $C_R = C_\alpha/C_\beta = I_\alpha/I_\beta$. Therefore, if we know the bulk concentration of the element, the volumes of the two phases (as measured from electron micrographs), and the intensity ratio, we can use Equation (1) to determine C_β and the relation $C_\alpha = C_R C_\beta$ to determine C_α.

The above scheme for analyzing lamellar intergrowths in effect uses the bulk composition of the intergrowth as its own internal standard. Its accuracy therefore relies on the assumption that the composition of the small area examined in the TEM is the same as that measured by electron microprobe. In the case of wonesite, multiple electron microprobe analyses yielded very similar compositions, suggesting that the wonesite is, in fact, quite homogeneous (Spear *et al.*, 1981) and that this anlaysis scheme might produce realistic compositions.

To simplify the analysis, we can assume that the wonesite exsolved talc with a composition that is collinear with the wonesite bulk composition and $Mg_3Si_4O_{10}(OH)_2$; this assumption is consistent with the composition of the talc crystals that coexist with the wonesite (Fig. 8). This has the effect of treating wonesite as a binary solid solution between talc and the composition $(Ca_{.004}Na_{.841}K_{.155})_{1.000}(Mg_{1.285}Fe_{.809}Mn_{.004}Cr_{.009}Ti_{.079}Al_{.660})_{2.846}[Al_{1.634}Si_{2.366}]_{4.000}O_{10}(OH,F)_2$. This composition is projected on Figure 8 as the point "E." Taking $C_s = 0.47$ (*e.g.*, the interlayer occupancy of bulk wonesite), the volume fraction of talc in the area from which the analyses were taken $V_{tc} = 1/4$, and using the intensity ratio of the aluminum peaks $I^{Al}_{tc}/I^{Al}_{wo} = 1/8$, equation (1) gives the concentration values $C_{tc} = 0.08$ and $C_{wo} = 0.60$ (normalized so that the talc end member would have C = 0.00 and the end member "E" would have C = 1.00).

The compositions of the talc and mica lamellae are shown as stars on Figure 8. This information also can be plotted on a temperature composition diagram of the join talc-"E" (Fig. 9). On this diagram, the bulk wonesite and talc compositions from Spear *et al.* (1981) are plotted at approximately 535°C (their estimate of the metamorphic temperature was 485–535°C; further work has suggested that the 535°C temperature is to be favored—Frank Spear, pers. comm.). The compositions of the mica and talc lamellae determined above are plotted as stars. Since they are exsolution lamellae, they clearly represent a lower temperature or range of temperatures than that of the peak metamorphism, but it is not possible to quantify

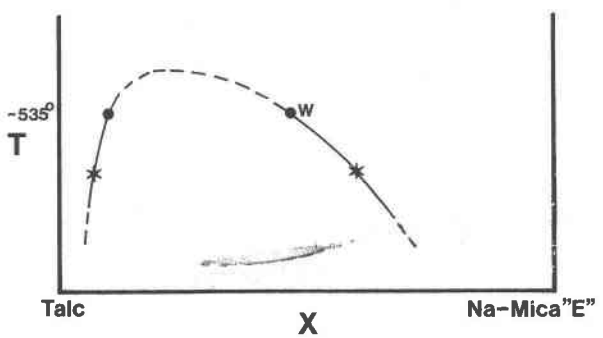

Fig. 9. A schematic temperature-composition (*T–X*) diagram showing the talc–wonesite miscibility gap. The Na-mica composition "E" is shown in Figure 8. Circles represent the bulk wonesite ("W") and talc compositions obtained by microprobe analysis by Spear *et al.* (1981); these are primary crystallization compositions representing a temperature of approximately 535°C. The compositions "*" were derived from the individual talc and wonesite exsolution lamellae by analytical TEM methods, as discussed in the text. The analyses are consistent with a misciblity gap skewed strongly toward talc.

Table 1. Compositions, hydration behavior, and interplanar spacings d_{001} of selected sodium micas and talc

Mineral	Reference	Composition	Expandable?	d_{001}
Na-phlogopite natural	Schreyer et al. (1980)	*	Yes**	?
Na-phlogopite synthetic	Carman (1974)	$NaMg_3[AlSi_3O_{10}](OH)_2$	Yes	9.90A
Na-eastonite synthetic	Franz and Althaus (1976)	$NaMg_{2.5}Al_{0.5}[Al_{1.5}Si_{2.5}O_{10}](OH)_2$	Yes	9.61
Preiswerkite natural	Keusen and Peters (1980)	*	No	9.67
Preiswerkite synthetic	Franz and Althaus (1976)	$NaMg_2Al[Al_2Si_2O_{10}](OH)_2$	No	9.68
Preiswerkite synthetic	Hewitt and Wones (1975)	$NaMg_2Al[Al_2Si_2O_{10}](OH)_2$	Yes	9.65
Wonesite natural	Spear et al. (1981)	*	***	9.57
Paragonite synthetic	Eugster et al. (1972)	$NaAl_2[AlSi_3O_{10}](OH)_2$	No	9.63
Talc natural	Perdikatsis and Burzlaff (1981)	$Mg_3[Si_4O_{10}](OH)_2$	No	9.35

* Compositions of natural specimens given in footnote 1.
** Expandability of the Schreyer et al. (1980) specimen was reported by Keusen and Peters (1980).
*** It is not known whether or not pure wonesite is expandable, because the existing specimen is intergrown with talc. However, on structural grounds, it is likely that wonesite is expandable.

this temperature. The critical temperature for the gap may be near 600°C, by analogy with the anthophyllite–gedrite solvus (Spear, 1980). The asymmetric form of the miscibility gap is to be expected: the steeper limb is on the side associated with the smaller cation (in this case a vacancy), while the gentler limb is on the side of the larger cation (Na).

Hydration properties of sodium micas

The fact that wonesite does not expand in water or ethylene glycol can be explained easily by the inclination of the exsolution lamellae with respect to (001). Talc is not an expandable mineral, and the slabs of talc cutting across the layers presumably hold them together physically. Under the temperature and pressure conditions of formation, homogeneous wonesite presumably was also unexpandable.

While the non-expandability of talc, as a result of close approach and van der Waals bonding of TOT layers of the structure, is well known, the question of which sodium-rich mica compositions are expandable is a confusing one. Table 1 presents chemical compositions, hydration properties (expandability), and interplanar spacings d_{001} reported for selected natural and synthetic sodium-rich micas and talc. From these data, it appears that even sodium trioctahedral micas with full interlayer sites are expandable, except in compositions with a large amount of tschermaks substitution. For these highly aluminous compositions (preiswerkites), there is a discrepancy in the expandability data; natural preiswerkite and the synthetic of Franz and Althaus (1976) do not expand in water, while the synthetic of Hewitt and Wones (1975) does. This difference may indicate that there is some unrecognized compositional difference between the two synthetics.

It is not immediately apparent why the aluminous sodium micas (preiswerkite and paragonite) generally do not expand, while less aluminous ones exhibit rapid expansion in water. Likewise, it is not clear why sodium biotites are expandable but potassium biotites are not. One obvious explanation is that the interlayer bonding involving sodium is weaker than that with potassium. It is alternatively possible, however, that the expandable synthetic sodium micas are deficient in sodium, containing substantial numbers of vacancies in the interlayer sites. Such solid solution toward talc, as found in the natural sodium micas wonesite and phlogopite of Schreyer *et al.* (1980), could explain the expandability discrepancy in preiswerkite; it would also be difficult to recognize in the fine-grained products of mica synthesis runs.

Table 1 also shows that most sodium micas have interplanar spacings d_{001} (based on a one-layuer mica cell) between 9.6Å and 9.7Å. Talc clearly has a smaller spacing at 9.35Å, while wonesite is 9.57Å. The slightly smaller d_{001} of wonesite may result from the large number of interlayer vacancies or from the data being collected from a mica-talc mixture. A major anomaly is the d_{001} = 9.90Å of the synthetic Na-phlogopite of Carman (1974). Possibly this mica had already expanded partially when the diffraction experiment was performed, or perhaps the measurement is in error. A determination of d_{001} of the mica of Schreyer *et al.* (1980) would provide a useful comparison with Carman's material.

In summary, the hydration properties of sodium-rich

micas are not fully understood. Expandability may be a function of aluminum content and may result largely from the different bonding characteristics of sodium, as compared to potassium. However, some of the observed hydration could also result from high concentrations of interlayer vacancies in synthetic sodium micas. In the future, electrostatic calculations of interlayer bonding energies might shed some light on the compositional dependencies of mica hydration.

Nomenclature of sodium micas

The talc-mica exsolution features in wonesite demonstrate clearly that the wonesite of Spear *et al.* (1981) is, indeed, a homogeneous mineral under metamorphic crystallization conditions, rather than being a mechanical mixture, for example. However, the exsolution does raise some questions about the nomenclature of sodium-rich micas. For example, what should we call the mica that was formed in the wonesite during the exsolution process? As can be seen in Figure 8, this mineral still is chemically close to the wonesite composition as it was originally defined by Spear *et al.* (1981). Furthermore, it is now obvious that micas in the interior of the ternary diagram of Figure 8 are solid solutions and that wide variations in composition are possible. Logically, the mica that has formed by exsolution of wonesite should also be called wonesite, even though it is a bit more sodic and aluminous than the "type" composition.

Preiswerkite and Na-phlogopite or Na-biotite appear to be reasonable end member names, but the compositional ranges to which these names apply are ambiguous. This ambiguity should be resolved, probably by the International Mineralogical Association. At present, it is not clear what we should call the mica of Schreyer *et al.* (1980); for example, is it Na-phlogopite or is it wonesite? Figure 8 shows that this mica, like wonesite, is really a ternary phase in the talc-preiswerkite-Na-biotite system, but that it is closer to the Na-end member than wonesite. Likewise, Figure 8 shows that wonesite should not be thought of simply as a talc-Na-biotite solid solution; the end member composition "E" is closer to preiswerkite than to the Na-biotite end member. Perhaps the name wonesite should be extended to include compositions, like "E," that are indicative of full interlayer sites and intermediate between preiswerkite and Na-biotite. On the other hand, perhaps "wonesite" should be reserved for sodium trioctahedral micas with substantial deficiencies in alkali cations. A reasonable nomenclature will also have to be consistent with the fact that sodium micas can absorb substantial amounts of the dioctahedral-trioctahedral substitution Al_2Mg_{-3} (note that the octahedral cation sum of wonesite is 2.94, rather than the ideal trioctahedral 3.0).

Relationships of mica and amphibole exsolution

Although exsolution phenomena have not been recognized previously in micas, exsolution has been recognized in numerous amphibole occurrences (Ghose, 1981; Robinson *et al.*, 1982). To understand the relationships between mica and amphibole exsolution and the miscibility gaps that cause the unmixing, it is instructive to treat the amphibole structures as consisting of mixtures of pyroxene-like structure and mica-like structure, as shown by Thompson (1970, 1978, 1981).

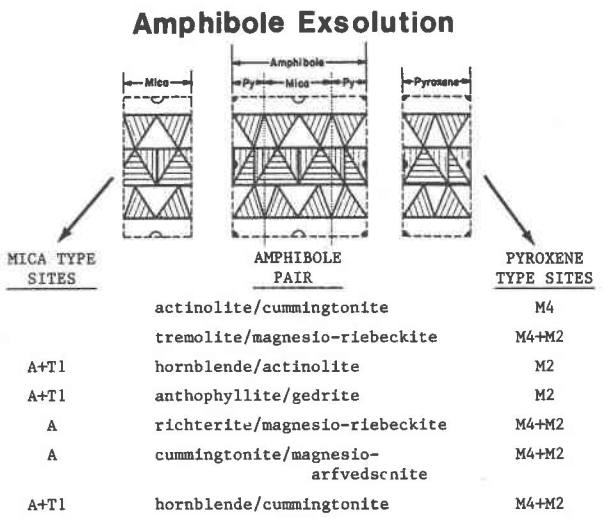

Fig. 10. Diagram showing which parts of the amphibole structure participate in various amphibole exsolution phenomena. Although some amphibole exsolution pairs differ chemically only in the pyroxene part of the structure, most amphibole immiscibility also involves the mica part of the structure. The portion of the figure illustrating the mica and pyroxene modules is from Thompson (1978).

Figure 10 shows one "I-beam" of amphibole, broken into its pyroxene and mica components. By examining the compositions of amphibole exsolution pairs, it is possible to determine which crystallographic sites are responsible for the immiscibility. Figure 10 lists several observed exsolution pairs, with the sites involved in the immiscibility apportioned to the mica and pyroxene parts of the amphibole structure (the site nomenclature refers to amphibole). Some types of exsolution, such as the pair actinolite-cummingtonite, involve only sites in the pyroxene part of the structure. In fact, these types of exsolution are also observed to occur in natural pyroxenes. For example, actinolite-cummingtonite exsolution, which is driven by Ca *vs.* Mg+Fe immiscibility in the amphibole M4 site, is entirely analogous to augite-pigeonite exsolution, which is also driven by Ca *vs.* Mg+Fe immiscibility in the pyroxene M2 site (M4 of amphibole is analogous to M2 of pyroxene).

Figure 10 shows that whereas some types of amphibole exsolution involve only the pyroxene part of the structure, other pairs involve sites in both the mica and pyroxene parts. In fact, in some pairs, such as anthophyllite-gedrite, it might be argued on crystal-chemical

grounds that it is the amphibole A-site that is causing the immiscibility and that the pyroxene-like sites are passively involved in the exsolution to fulfill charge balance requirements. The amphibole exsolution phenomena that involve the mica-like part of the structure all involve the A-site, which is analogous to the interlayer site of micas, and they all involve immiscibility of one amphibole with an A-site that is more-or-less empty and one with an A-site that is more full. This is also precisely the case in wonesite: one phase with an interlayer site that is more-or-less empty (talc) exsolves from another phase that has a fuller interlayer site.

The recognition of immiscibility between talc and wonesite (Spear *et al.*, 1978, 1981; Thompson, 1981) and of exsolution of wonesite to a lamellar intergrowth of talc and Na-mica thus presents us with a symmetrical way of viewing exsolution in amphiboles. Some exsolution involves the pyroxene part of the structure, and the analogous behavior is observed in pyroxenes. Likewise, some exsolution involves the mica part of the structure, and the analogous behavior is observed in the mica wonesite. These analogies testify to the strength of the polysomatic model for biopyriboles: it appears that analogous crystallographic sites behave the same way chemically, regardless of the biopyribole structure in which they reside.

And, with hindsight. . .

The TEM study described above clarifies a number of observations that has been made in the original X-ray, chemical, and textural study of wonesite. Frank Spear has very kindly consented to the presentation of these clarifications in the present paper, and he generously made available to me primary data from the original wonesite study (Spear *et al.*, 1978, 1981). In hindsight, knowing that wonesite is a lamellar intergrowth of sodium mica and talc, the following observations can be made:

1. Powder X-ray diffraction patterns of sheet silicates in the specific specimen described in this study invariably indicated the presence of talc, even though no talc could be observed petrographically. This is clearly because the wonesite contained the unrecognized talc lamellae.

2. In crossed polarized light, some crystals of wonesite exhibit a curious wavy pattern, somewhat like that in Figure 5, that is not characteristic of other sheet silicates. Although the origin of this lamellar feature was originally not understood, it is almost certainly the optical manifestation of the talc and mica exsolution lamellae.

3. The X-ray precession photographs of wonesite are of very poor quality, as noted by Spear *et al.* (1981), due to twinning, stacking disorder, and crystal deformation. Careful examination of 00*l* diffractions does, however, reveal that they are split in a fashion similar to the splitting in the electron diffraction pattern of Figure 2. Measurement of the films indicates that the two sets of diffraction maxima result from talc and sodium mica. This type of splitting could easily be confused with splitting due to the presence of both the $K\alpha_1$ and $K\alpha_2$ X-ray wavelengths.

The above reinterpretations of the X-ray and optical data indicate that these observations are wholly consistent with the results of the TEM study.

Conclusions

The separation of talc and sodium mica in wonesite provides the first clear example of exsolution in a mica. In addition, this phenomenon is a direct analogy for types of amphibole exsolution that involve the mica-like part of the amphibole structure.

This study also emphasizes the value of combining imaging techniques with the analytical capabilities of modern TEM's in studies of complex mineral intergrowths. Where other methods were unable to precisely define the nature of wonesite, electron microscopy has clarified the physical and chemical state of this mica. In so doing, this TEM study supports the earlier X-ray and chemical studies that defined wonesite as a new mineral.

This investigation also raises the possibility of exsolution in other micas. Although the degree of solid solution of potassium micas toward talc is much more limited than that of wonesite, it is possible that small volumes of talc (or pyrophyllite) could exsolve from biotites and muscovites, for example. In the future, electron microscopists studying micas, as well as petrologists, should at least be alert to this possibility.

Acknowledgments

Dr. Frank S. Spear kindly provided specimens of wonesite from the type locality and made available data from the pioneering wonesite study. The following are thanked for helpful discussions or comments: Drs. David L. Bish, Charles W. Burnham, Robert M. Hazen, Frank S. Spear, and James B. Thompson, Jr. This work was supported by NSF Grants EAR-8115790 and EAR-8009242. Electron microscopy was performed in the Arizona State University Facility for High Resolution Electron Microscopy, which was established with support from the NSF Regional Instrumentation Facilities Program, Grant CHE-7916098.

References

Amouric, M., Mercuriot, G., and Baronnet, A. (1981) On computed and observed HRTEM images of perfect mica polytypes. Bulletin de Mineralogie, 104, 298–313.

Bollman, W. (1970) Crystal Defects and Crystalline Interfaces. Springer-Verlag, New York.

Buseck, P. R. and Veblen, D. R. (1981) Defects in minerals as observed with high-resolution transmission electron microscopy. Bulletin de Mineralogie, 104, 249–260.

Carman, J. H. (1974) Synthetic sodium phlogopite and its two hydrates: stabilities, properties, and mineralogic implications. American Mineralogist, 59, 261–273.

Eugster, H. P., Albee, A. L., Bence, A. E., Thompson, J. B., Jr. and Waldbaum, D. R. (1972) The two-phase region and excess mixing properties of paragonite-muscovite crystalline solutions. Journal of Petrology, 13, 147–179.

Franz, G. and Althaus, E. (1976) Experimental investigation on

the formation of solid solutions in sodium–magnesium micas. Neues Jahrbuch für Mineralogie, Abhandlungen, 126, 233–253.

Ghose, S. (1981) Subsolidus reactions and microstructures in amphiboles. In D. R. Veglen, Ed., Reviews in Mineralogy, 9A, Amphiboles and Other Hydrous Pyriboles—Mineralogy, p. 325–372. Mineralogical Society of America, Washington, D. C.

Hazen, R. M. and Finger, L. W. (1978a) The crystal structures and compressibilities of layer minerals at high pressure. I. SnS_{22}, berndtite. American Mineralogist, 63, 289–292.

Hazen, R. M. and Finger, L. W. (1978b) The crystal structures and compressibilities of layer minerals at high pressure. II. Phlogopite and chlorite. American Mineralogist, 63, 293–296.

Hewitt, D. A. and Wones, D. R. (1975) Physical properties of some synthetic Fe–Mg–Al trioctahedral biotites. American Mineralogist, 60, 854–862.

Iijima, S. and Buseck, P. R. (1978) Experimental study of disordered mica structures by high-resolution electron microscopy. Acta Crystallographica, A34, 709–719.

Jaffe, H. W., Robinson P., Tracy, R. J., and Ross, M. (1975) Orientation of pigeonite lamellae in metamorphic augite: correlation with composition and calculated optimal phase boundaries. American Mineralogist, 60, 9–28.

Keusen, H. R. and Peters, Tj. (1980) Preiswerkite, an Al-rich trioctahedral sodium mica from the Geisspfad ultramafic complex (Penninic Alps). American Mineralogist, 65, 1134–1137.

Perdikatis, B. and Burzlaff, H. (1981) Structure refinement of talc $Mg_3[(OH)_2Si_4O_{10}]$. Zeitschrift für Kristallographie, 156, 177–186.

Reeder, R. J. (1981) Electron optical investigation of sedimentary dolomites. Contributions to Mineralogy and Petrology, 76, 148–157.

Robinson, P., Jaffe, H. W., Ross, M., and Klein, C. (1971) Orientation of exsolution lamellae in clinopyroxenes and clinoamphilboles: consideration of optimal phase boundaries. American Mineralogist, 56, 909–939.

Robinson, P., Ross, M., Nord, G. L., Jr., Smyth, J. R., and Jaffe, H. W. (1977) Exsolution lamellae in augite and pigeonite: fossil indicators of lattice parameters at high temperature and pressure. American Mineralogist, 62, 857–873.

Robinson, P., Spear, F. S., Schumacher, J. C., Laird, J., Klein, C., Evans, B. W., and Doolan, B. L. (1982) Phase relations of metamorphic amphiboles: natural occurrence and theory. In D. R. Veblen and P. H. Ribbe, Eds., Reviews in Mineralogy, 9B, Amphiboles: Petrology and Experimental Phase Relations, p. 1–228. Mineralogical Society of America, Washington, D. C.

Schreyer, W., Abraham, K., and Kulke, H. (1980) Natural sodium phlogopite coexisting with potassium phlogopite and sodian aluminian talc in a metaphoric evaporite sequence from Derrag, Tell Atlas, Algeria. Contributions to Mineralogy and Petrology, 74, 223–233.

Spear, F. S. (1980) The gedrite–anthophyllite solvus and the composition limits of orthoamphibole from the Post Pond Volcanics, Vermont. American Mineralogist, 65, 1103–1118.

Spear, F. S., Hazen, R. M., and Rumble D., III (1978) Sodium trioctahedral mica: a possible new rock-forming silicate from the Post Pond Volcanics, Vermont. Carnegie Institution of Washington Year Book, 77, 808–812.

Spear, F. S., Hazen, R. M., and Rumble D., III (1981) Wonesite: a new rock-forming silicate from the Post Pond Volcanics, Vermont. American Mineralogist, 66, 100–105.

Thompson, J. B., Jr. (1970) Geometrical possibilities for amphibole structures: Model biopyriboles. (abstr.) American Mineralogist, 55, 292–293.

Thompson, J. B., Jr. (1978) Biopyriboles and polysomatic series. American Mineralogist, 63, 239–249.

Thompson, J. B., Jr. (1981) An introduction to the mineralogy and petrology of the biopyriboles. In D. R. Veblen, Ed., Reviews in Mineralogy, 9A, Amphiboles and Other Hydrous Pyriboles—Mineralogy, p. 141–188. Mineralogical Society of American, Washington, D. C.

Tullis, J. and Yund, R. A. (1979) Calculation of coherent solvi for alkali feldspar, iron-free clinopyroxene, nepheline–kalsilite, and hematite–ilmenite. American Mineralogist, 64, 1063–1074.

Veblen, D. R. (1980) Anthophyllite asbestos: microstructures, intergrown sheet silicates, and mechanisms of fiber formation. American Mineralogist, 65, 1075–1086.

Veblen, D. R. (1983) Microstructures and mixed layering in intergrown wonesite, chlorite, talc, biotite, and kaolinite. American Mineralogist, 68, 566–580.

Veblen, D. R. and Buseck, P. R. (1979) Serpentine minerals: intergrowths and new combination structures. Science, 206, 1398–1400.

Veblen, D. R. and Buseck, P. R. (1980) Microstructures and reaction mechanisms in biopyriboles. American Mineralogist, 65, 599–623.

Veblen, D. R. and Buseck, P. R. (1981) Hydrous pyriboles and sheet silicates in pyroxenes and uralites: intergrowth microstructures and reaction mechanisms. American Mineralogist, 66, 1107–1134.

Willaime, C. and Brown, W. L. (1974) A coherent elastic model for the determination of the orientation of exsolution boundaries: application to the feldspars. Acta Crystallographica, A30, 316–331.

Manuscript received, April 30, 1982;
accepted for publication, October 11, 1982.